Journal of ELECTRONIC MATERIALS, Vol. 42, No. 12, 2013
DOI: 10.1007/s11664-013-2817-3
© 2013 TMS

Effects of Y_2O_3 Nanoparticles on Growth Behaviors of Cu_6Sn_5 Grains in Soldering Reaction

L.M. YANG[1,2,3,4] and Z.F. ZHANG[2,5]

1.—University of Science and Technology of China, 96 JinZhai Road, Hefei 230026, China. 2.—Shenyang National Laboratory for Materials Science, Institute of Metal Research, Chinese Academy of Science, 72 Wenhua Road, Shenyang 110016, China. 3.—Department of Physics, Shenyang University of Technology, 111 Shenliaoxi Road, Shenyang 110870, China. 4.—e-mail: lmyang10b@imr.ac.cn. 5.—zhfzhang@imr.ac.cn

The effects of Y_2O_3 nanoparticles doped in Sn-3Ag-0.5Cu solder on the growth behaviors of Cu_6Sn_5 grains in the soldering reaction with copper were investigated. It is found that the growth rate of Cu_6Sn_5 grains was markedly decreased due to the addition of Y_2O_3 nanoparticles. The statistical size distribution results indicated that Cu_6Sn_5 grains with radius less than the average value account for a high percentage. These results confirm that the nanoparticles can effectively suppress the diffusion behaviors of Cu atoms in the wetting reaction.

Key words: Lead-free solder, intermetallic compounds, interfacial reaction, grain growth

INTRODUCTION

Solder joints between the lead frame of chips and the circuit board, providing not only mechanical connections but also current paths in service, are crucial to electronic packaging. Traditionally, tin-lead alloy has been widely used as a solder material. However, many electronic manufacturers have stepped up their search for new lead-free solders to substitute tin-lead alloys due to health and environmental concerns.[1] The reliability of new lead-free solder has become an interesting research focus.[2–7] To enhance the reliability of solder joints, numerous investigations have been performed, such as adding rare-earth elements, nanoparticles, and other metallic elements into solder materials.[8–10] Although there have been some studies on lead-free solder doped with nanoparticles recently, they focused mainly on isothermal aging or the mechanical properties of the doped solder itself.[11–13] Few reports to date have considered the mechanism of interfacial reaction or the properties of the interfaces between nanoparticle-doped solder and the substrate.

During the reflow soldering process, intermetallic compounds are formed between the solder and the substrate. Generally, the intermetallic compound layer between lead-free solder and Cu substrate is dominantly composed of Cu_6Sn_5 compound.[14] In addition, Cu_3Sn intermetallic compound can be detected, but only when the reflow temperature is very high or the aging time is long enough.[15] The size, morphology, and thickness of the Cu_6Sn_5 intermetallic compound have a notable influence on the reliability of solder joints, since fracture always occurs near intermetallic compounds at interfaces.[16–19] Cu_6Sn_5 grains of large size, which normally endure higher stress in comparison with those of small size, are more apt to fracture prior to the solder.[20] Therefore, it is necessary to understand the growth kinetics mechanism and control the growth of intermetallic compounds between solder and substrate.

On the other hand, the classical theory of conservative ripening of precipitates by Lifshitz and Slyozov[21] and Wagner[22] (LSW theory) is not suitable for nonconservative ripening of Cu_6Sn_5 grains in the wetting reaction.[21,22] In 2002, Gusak and Tu[23] proposed a new flux-driven ripening (FDR)

(Received May 2, 2013; accepted September 23, 2013; published online October 17, 2013)

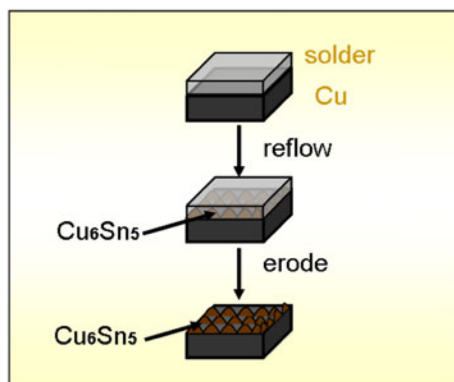

Fig. 1. Schematic illustration of the experimental process for Cu_6Sn_5 morphology observation.

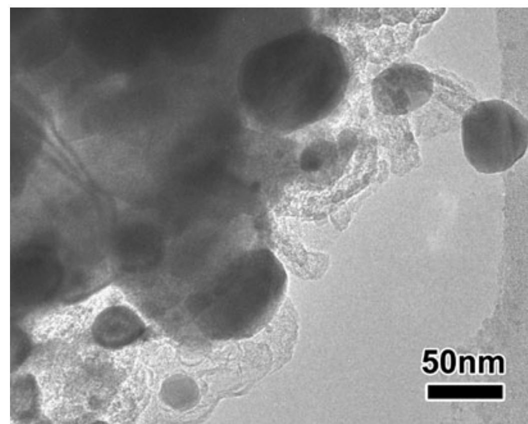

Fig. 2. Transmission electron microscopy image of Y_2O_3 nanoparticles.

theory to predict the size distribution of Cu_6Sn_5 grains with scallop shape and the rate of change of the average size $\langle r \rangle$ with the wetting reaction time t, namely that $\langle r \rangle$ is proportional to $t^{1/3}$, which was proved to agree perfectly with experimental statistical results for Cu_6Sn_5 grains by other researchers.[24,25] In this study, the growth rate of the average size of Cu_6Sn_5 grains with the wetting time is found to be greatly decreased by addition of Y_2O_3 nanoparticles to Sn-3Ag-0.5Cu solder, compared with the solder without nanoparticle doping.

EXPERIMENTAL PROCEDURES

Cold-drawn polycrystalline Cu was selected as the substrate, and Sn-3Ag-0.5Cu (wt.%) or Sn-3Ag-0.5Cu doped with Y_2O_3 nanoparticles (0.1 wt.%) was used as the solder material. Firstly, Y_2O_3 nanoparticles were prepared by the combustion method, as reported previously in detail.[26] The nanoparticles were dissolved in ethanol and ultrasonicated to avoid agglomeration. The dispersed Y_2O_3 nanoparticles were mixed homogeneously with Sn-3Ag-0.5Cu solder paste. Secondly, the Cu substrates were ground with 800#, 1200#, and 2000# SiC emery paper and polished carefully with diamond polishing pastes. Thereafter, Sn-3Ag-0.5Cu solder paste or the Sn-3Ag-0.5Cu solder doped with Y_2O_3 nanoparticles was spread onto the surface of polished Cu. All solder/Cu samples were placed into an oven at constant temperature at 240°C for 2 min, 5 min, 15 min, and 20 min, followed by cooling in air to room temperature. Finally, the reacted samples were deep etched with 5% HCl + 3% HNO_3 + CH_3OH (vol.%) etchant solution to remove excess solder so that the Cu_6Sn_5 grains were completely exposed. The preparation process is shown in Fig. 1. The morphologies of Cu_6Sn_5 on the interface were observed using a LEO Supra 35 scanning electron microscope (SEM). The size distribution based on a large number of Cu_6Sn_5 grains was measured using Image-Pro Plus software.

RESULTS AND DISCUSSION

Figure 2 shows a transmission electron microscopy (TEM) image of Y_2O_3 nanoparticles added into the Sn-3Ag-0.5Cu solder. Spherical particles in the micrograph represent Y_2O_3 nanoparticles, and the diameters of these particles are not very homogeneous. The size of most nanoparticles is about 30 nm, but a few particles have diameter close to 70 nm, as measured by Image-Pro Plus. There are two reasons for the selection of the Y_2O_3 nanoparticles as dopant: one is that Y_2O_3 nanoparticles do not react with any atoms of the substrate or solder, and the other is their excellent thermal stability. The diameter of the Y_2O_3 nanoparticles prepared by the combustion method did not obviously increase even when aged at 500°C.[26]

Figure 3a, b, and c show top-view images of Cu_6Sn_5 grains formed in the reaction between Sn-3Ag-0.5Cu solder and Cu for 2 min, 5 min, and 15 min, respectively. Figure 3d–f display corresponding images of Cu_6Sn_5 grains formed by Y_2O_3-nanoparticle-doped Sn-3Ag-0.5Cu solder and Cu. It can be seen that scallop-shaped Cu_6Sn_5 intermetallic compound grains, as confirmed by energy-dispersive spectrometry (EDS), appear between the solder and Cu substrate after reflow. The size of the Cu_6Sn_5 grains increased markedly with increasing reflow time for the Sn-3Ag-0.5Cu solder, as shown in Fig. 3a–c. However, there was only a slight increase in size for the Cu_6Sn_5 grains formed by the nanoparticle-doped solder and Cu substrate (Fig. 3d–f), indicating an obvious suppression effect on the growth of the Cu_6Sn_5 grains by doping with Y_2O_3 nanoparticles.

Based on the measured size distribution of the Cu_6Sn_5 grains, the relationship between the average radius of the Cu_6Sn_5 grains and the reflow time is shown in Fig. 4a. The data for the Cu_6Sn_5 grains formed by Sn-3Ag-0.5Cu solder and Cu can be fit appropriately by a line with slope of $k_1 = 1/3$ in logarithmic coordinates. Thus, the average radius

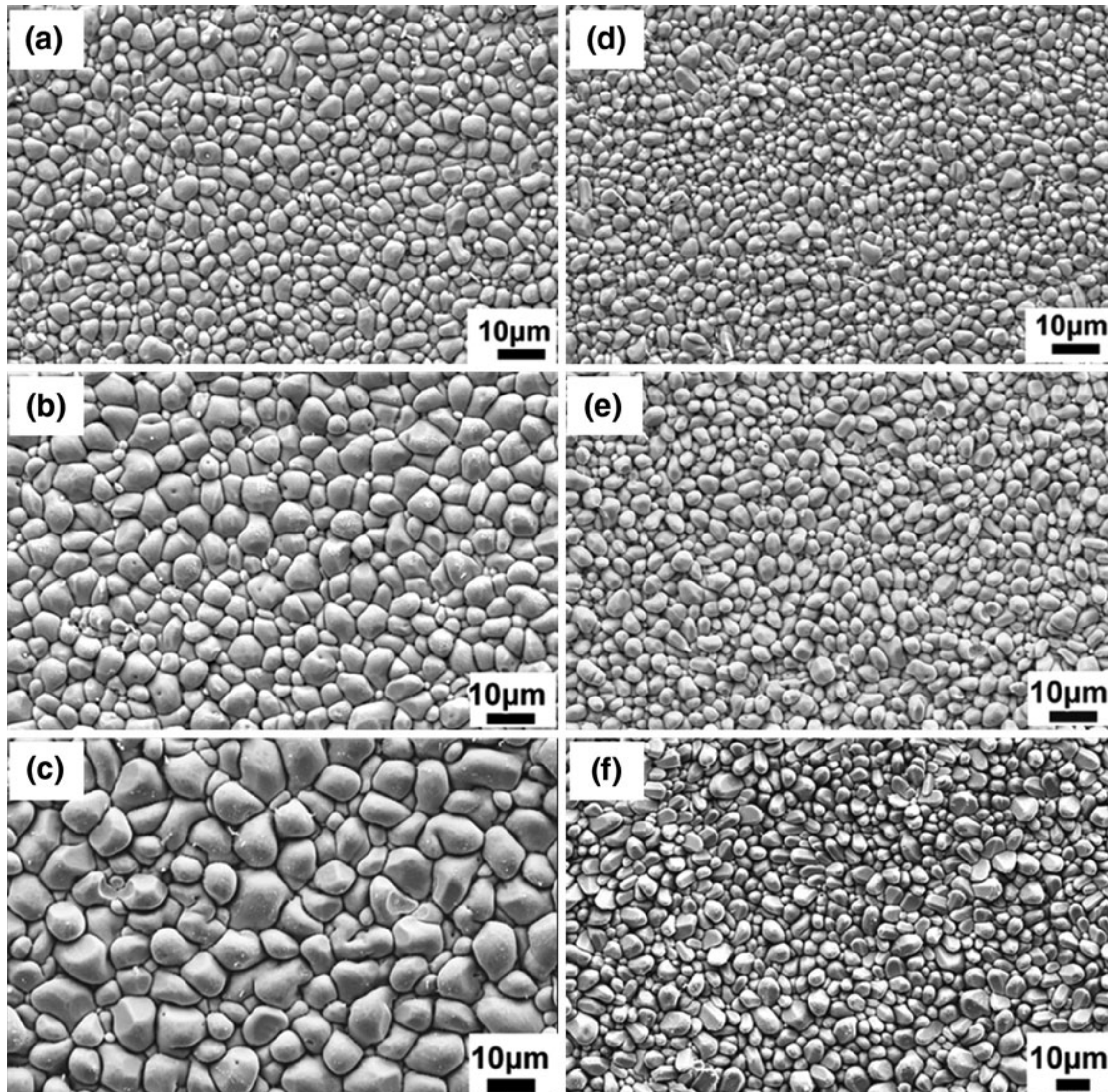

Fig. 3. Top-view scanning electron microscopy images of Cu_6Sn_5 formed by the reaction between Cu and: Sn-3Ag-0.5Cu solder for (a) 2 min, (b) 5 min, and (c) 15 min, and Y_2O_3-nanoparticle-doped Sn-3Ag-0.5Cu solder for (d) 2 min, (e) 5 min, and (f) 15 min.

$\langle r \rangle$ increases with the reflow time t according to the equation

$$\langle r \rangle = C_1 t^{1/3}, \tag{1}$$

where C_1 is a constant. The rate of increase of the average radius with reflow time is in accordance with the FDR theory and the experimental results by others.[23–25] However, the average radius of Cu_6Sn_5 formed in the wetting reaction between Y_2O_3-nanoparticle-doped solder and Cu increased with reflow time according to the equation

$$\langle r \rangle = C_2 t^{1/6}, \tag{2}$$

where C_2 is another constant. This indicates that addition of Y_2O_3 nanoparticles to Sn-3Ag-0.5Cu solder could effectively suppress the growth of Cu_6Sn_5 intermetallic compound. Figure 4b, c, and d shows the size distribution of Cu_6Sn_5 grains formed in the soldering reaction between Y_2O_3-nanoparticle-doped solder and Cu. The frequency in Fig. 4b, c, and d gives the normalized number percentage of Cu_6Sn_5 grains, and $r/\langle r \rangle$ indicates the ratio of each radius r of Cu_6Sn_5 grains to the average radius $\langle r \rangle$. It is indicated that the Y_2O_3 nanoparticles have an obvious effect on the size distribution of Cu_6Sn_5. However, the FDR theory curve cannot exactly fit our experiment results. The distribution peaks in Fig. 4b, c, and d all shift to the left, even to abscissa values less than 1.0, meaning that Cu_6Sn_5 grains with radius less than the average radius $\langle r \rangle$ account for a greater percentage due to the addition of the Y_2O_3 nanoparticles to the solder.

Figure 5a, b, and c show cross-sectional images of interfacial compounds formed between Sn-3Ag-0.5Cu solder and Cu after 2 min, 5 min, and 15 min,

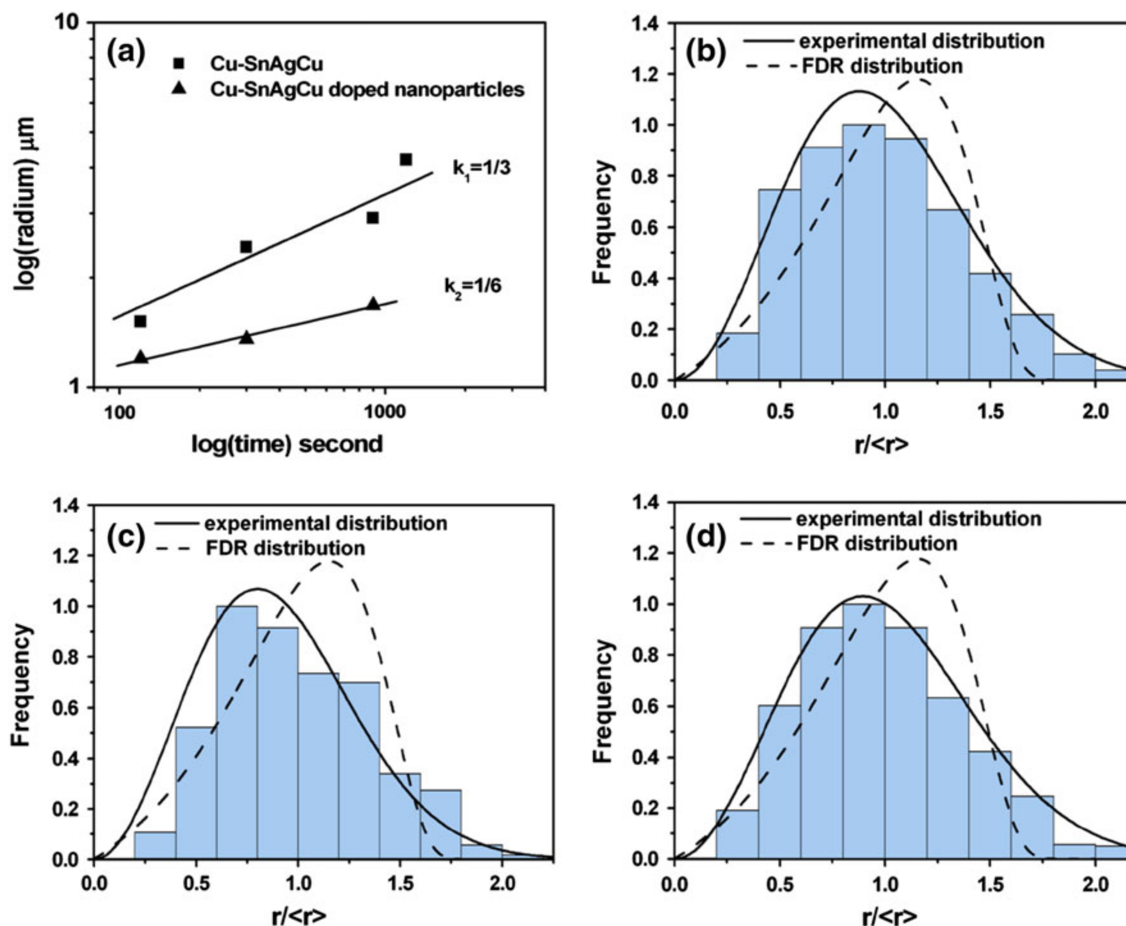

Fig. 4. (a) Relationship between average radius of Cu_6Sn_5 grains and reflow time. Size distributions of Cu_6Sn_5 grains formed by Y_2O_3-nanoparticle-doped Sn-3Ag-0.5Cu solder and copper after different reflow times: (b) 2 min, (c) 5 min, and (d) 15 min.

respectively; Fig. 5d, e, and f show images of interfacial compounds formed between Y_2O_3-nanoparticle-doped Sn-3Ag-0.5Cu solder and Cu after 2 min, 5 min, and 15 min, respectively. With the increase of reflow time, the layer of interfacial intermetallic compounds mainly composed of Cu_6Sn_5 became obviously thicker. It should be noted that a few Cu_6Sn_5 grains evolved into a prism shape with increasing reflow time for the nanoparticle-doped Sn-Ag-Cu solder, meaning that their size perpendicular to the interface is larger than that parallel to the interface. The mean thickness of the interfacial compound layer was calculated by dividing its area by its length. Figure 6 shows that the mean thickness of the intermetallic compounds increases as a function of reflow time. The thickness of interfacial compounds for the nanoparticle-doped solder is slightly smaller than for the undoped solder for given reflow time.

The distribution of nanoparticles in the solder is shown in Fig. 7. The white dots in the micrograph denote nanoparticles. Since the Y_2O_3 nanopowder is noncompact and has low mass density, a small mass addition can result in a large volume distribution in the solder. The nanoparticles distributed in the solder should have an influence on the growth behaviors of the intermetallic compounds. Figure 8a demonstrates the growth mechanism of Cu_6Sn_5 grains in the reaction between molten solder and the copper substrate. There should be two paths for the formation of Cu_6Sn_5 intermetallic compound: One path is that Cu reacts with Sn at the Cu_6Sn_5/Sn interface, and another can occur at the interface between the molten Sn in channels and the Cu substrate. Due to the Gibbs–Thomson effect,[21] the concentration C of Cu in the molten solder at the surface of a Cu_6Sn_5 grain can be expressed as follows:

$$C = C_0 \exp\left(\frac{2\gamma V_{\mathrm{m}}}{rRT}\right), \tag{3}$$

where C_0 is the equilibrium concentration of Cu in the solder, γ is the interfacial energy per unit area between Cu_6Sn_5 and molten solder, V_{m} represents the molar volume of Cu_6Sn_5, R is the gas constant, T is the reflow temperature, and r is the radius of the Cu_6Sn_5 grain.[27,28] Equation (3) can be written as follows:

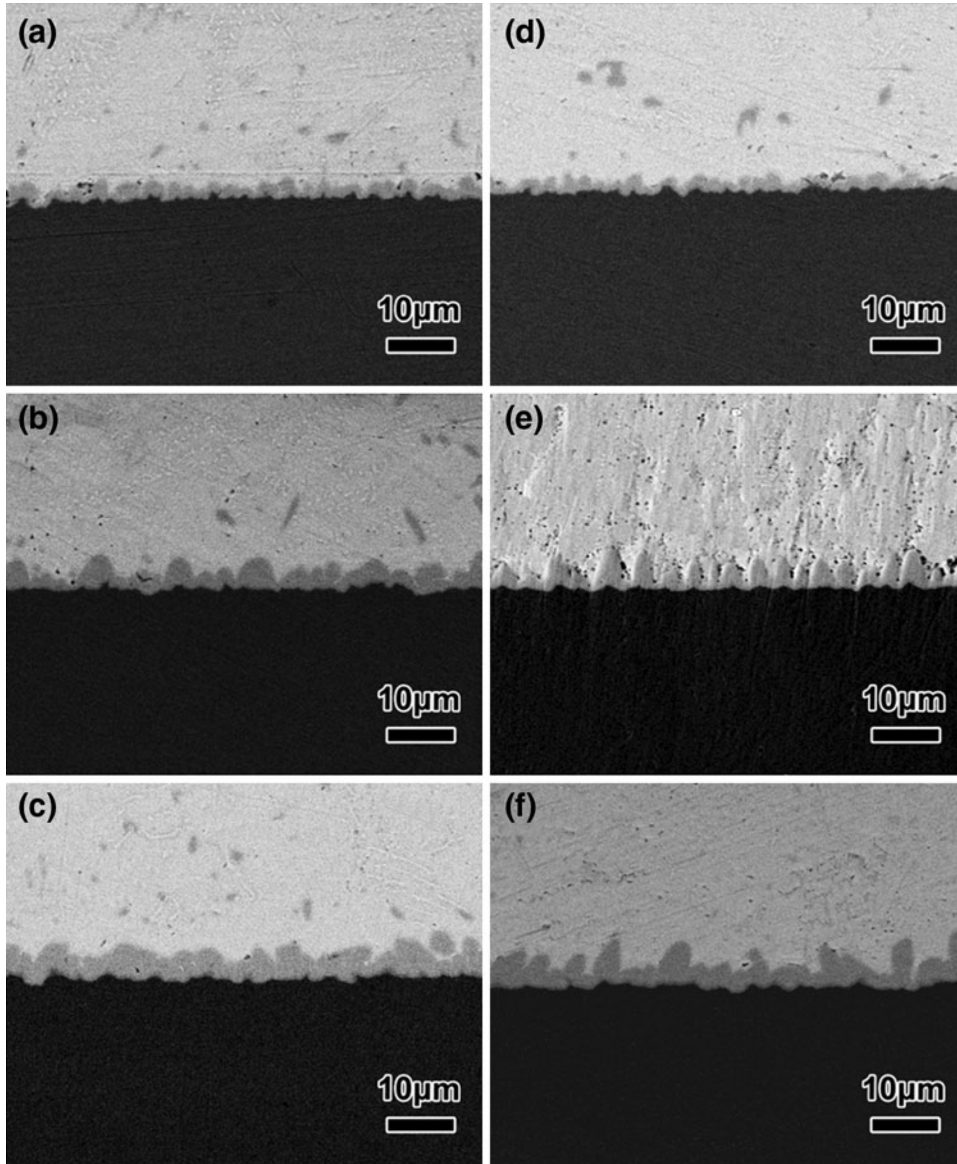

Fig. 5. Cross-sectional images of interfacial compounds formed between Cu and: Sn-3Ag-0.5Cu solder after (a) 2 min, (b) 5 min, and (c) 15 min, and Y_2O_3-nanoparticle-doped Sn-3Ag-0.5Cu solder after (d) 2 min, (e) 5 min, and (f) 15 min.

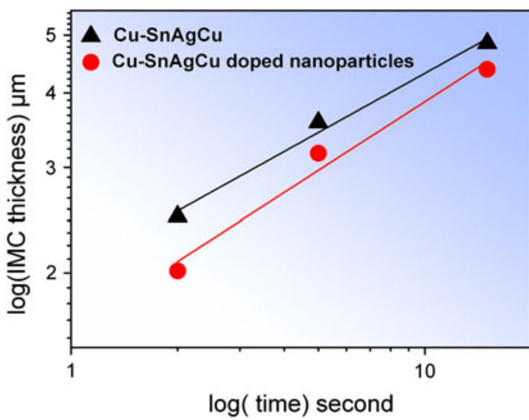

Fig. 6. Interfacial intermetallic compound thickness increase as a function of reflow time.

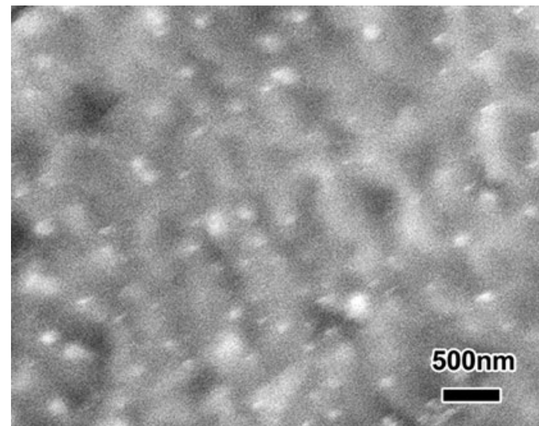

Fig. 7. SEM image of Sn-3Ag-0.5Cu solder doped with Y_2O_3 nanoparticles.

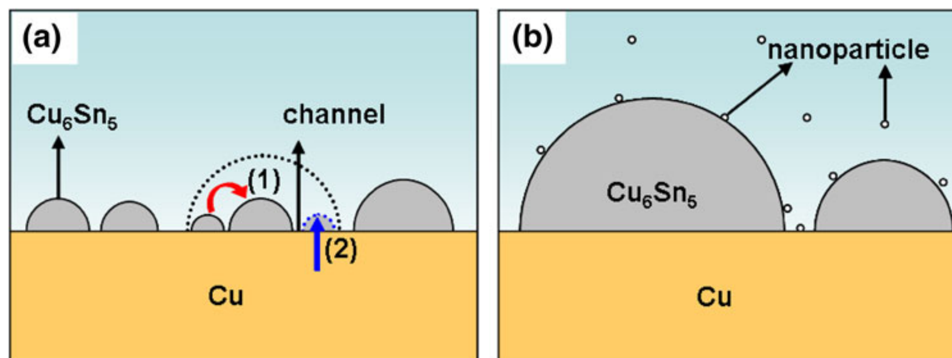

Fig. 8. (a) Growth paths of Cu_6Sn_5. (b) Sketch of the distribution of Y_2O_3 nanoparticles.

$$C \cong C_0\left(1+\frac{2\gamma V_m}{rRT}\right) \text{ if } \frac{2\gamma V_m}{rRT} << 1. \quad (4)$$

A concentration gradient of Cu is set up between grains of different radius, inducing diffusion of Cu atoms from small grains to large grains. This causes the large grains to grow and the small ones to shrink, as indicated by path (1) in Fig. 8a. According to Eq. (4), the diffusion flux J_1 of Cu atoms by path (1) can be expressed as follows:

$$J_1 = -D\frac{dC}{dx} \cong -\frac{2\gamma V_m C_0 D}{3LRTr^2}, \quad (5)$$

where L is a dimensionless coefficient and D is the Cu atom diffusion coefficient.[28] It is well known that the diffusion coefficient D can be expressed as

$$D = D_0 e^{-\frac{Q}{RT}}, \quad (6)$$

where D_0 is the equilibrium constant, R is the gas constant, T is the temperature, and Q is the activation energy for diffusion. The activation energy for diffusion is the minimum energy necessary for an atom to transfer from one position to another. In the solder doped with Y_2O_3 nanoparticles, the nanoparticles could adhere to the interface of Cu_6Sn_5 grains or lie in the solder as shown in Fig. 8b. These nanoparticles block the diffusion of some Cu atoms, which therefore require a higher energy to overcome these obstacles. This means that the activation energy for diffusion would be enhanced due to the addition of nanoparticles to the solder, decreasing the diffusion flux of Cu atoms in the solder during the reflow process. Another way of Cu_6Sn_5 grain growth is the reaction of molten solder in channels between Cu_6Sn_5 grains and the Cu substrate, as shown by path (2) in Fig. 8a. Since the transfer distance of Cu atoms in path (1) is longer than that in path (2), the influence of Y_2O_3 nanoparticles on the diffusion flux of path (1) is more prominent than for path (2). At the beginning of the wetting reaction, both path (1) and path (2) are important to the growth behavior of Cu_6Sn_5 grains. However, the contribution of path (2) receded notably as the channels shrink with increasing reflow time. Thus, diffusion by path (1), which could be obstructed by Y_2O_3 nanoparticles, distinctly dominated the growth of Cu_6Sn_5 grains for long reflow time. As a result, for the solder doped with Y_2O_3 nanoparticles, the growth of Cu_6Sn_5 grains could be suppressed in comparison with the solder that was not doped with nanoparticles.

CONCLUSIONS

The growth behaviors of Cu_6Sn_5 grains were markedly influenced by Y_2O_3 nanoparticles doped in solder. At the initial stage of the wetting reaction, the growth of Cu_6Sn_5 grains could be attributed to reactions at both the Cu_6Sn_5/Sn interface and the Cu substrate/Sn interface. With increasing reflow time, the reaction between Cu atoms diffusing from small Cu_6Sn_5 grains to larger ones and molten Sn at the Cu_6Sn_5/Sn interface became dominant. The diffusion process of Cu atoms could be blocked by Y_2O_3 nanoparticles in the composite solder, leading to marked suppression of the growth of Cu_6Sn_5 grains compared with the solder without Y_2O_3 nanoparticle doping.

ACKNOWLEDGEMENTS

The authors would like to thank Q.K. Zhang for his help in the experiments. This research was financially supported by the National Basic Research Program of China under Grant No. 2010CB631006.

REFERENCES

1. Y. Li, K. Moon, and C.P. Wong, *Science* 308, 1419 (2005).
2. Z.Z. Chen, N. Kioussis, K.N. Tu, N.G. Ghoniem, and J.M. Yang, *Phys. Rev. Lett.* 105, 015703 (2010).
3. J.Y. Kim and J. Yu, *Appl. Phys. Lett.* 92, 092109 (2008).
4. K.N. Tu, *Microelectron. Reliab.* 51, 517 (2011).
5. K.N. Tu, *J. Appl. Phys.* 94, 5451 (2003).
6. L.M. Yang, Q.K. Zhang, and Z.F. Zhang, *Scripta Mater.* 67, 637 (2012).
7. B. Chao, S.H. Chae, X.F. Zhang, K.H. Lu, J. Im, and P.S. Ho, *Acta Mater.* 55, 2805 (2007).
8. W.M. Xiao, Y.W. Shi, G.C. Xu, R. Ren, F. Guo, Z.D. Xia, and Y.P. Lei, *J. Alloys Compd.* 472, 198 (2009).

9. J.X. Wang, S.B. Xue, Z.J. Han, S.L. Yu, Y. Che, Y.P. Shi, and H. Wang, *J. Alloys Compd.* 467, 219 (2009).
10. J. Shen and Y.C. Chan, *Microelectron. Reliab.* 49, 223 (2009).
11. L.C. Tsao and S.Y. Chang, *Mater. Des.* 31, 990 (2010).
12. L.C. Tsao, *J. Alloys Compd.* 509, 8441 (2011).
13. P. Liu, P. Yao, and J. Liu, *J. Electron. Mater.* 37, 874 (2008).
14. H.F. Zou, H.J. Yang, and Z.F. Zhang, *Acta Mater.* 56, 2649 (2008).
15. H.F. Zou and Z.F. Zhang, *J. Appl. Phys.* 108, 103518 (2010).
16. S.W. Chen, S.W. Lee, and M.C. Yip, *J. Electron. Mater.* 32, 1284 (2003).
17. M.O. Alam, Y.C. Chan, and K.C. Hung, *Microelectron. Reliab.* 42, 1065 (2002).
18. J.W. Yoon, S.W. Kim, and S.B. Jung, *Mater. Trans.* 45, 727 (2004).
19. J.W. Yoon, S.W. Kim, and S.B. Jung, *J. Alloys Compd.* 385, 192 (2004).
20. Q.K. Zhang and Z.F. Zhang, *J. Appl. Phys.* 112, 064508 (2012).
21. I.M. Lifshitz and V.V. Slyozov, *J. Phys. Chem. Solids* 19, 35 (1961).
22. C.Z. Wagner, *Elektrochem* 65, 581 (1961).
23. A.M. Gusak and K.N. Tu, *Phys. Rev. B* 66, 115403 (2002).
24. J.O. Suh, K.N. Tu, G.V. Lutsenko, and A.M. Gusak, *Acta Mater.* 56, 1075 (2008).
25. J. Gö rlich, G. Schmitz, and K.N. Tu, *Appl. Phys. Lett.* 86, 053106 (2005).
26. L.M. Yang, S.Y. Quan, Y.D. Yang, and G.M. Shi, *J. Nanosci. Nanotechnol.* 12, 2700 (2012).
27. J.H. Yao, K.R. Elder, H. Guo, and M. Grant, *Phys. Rev. B* 47, 14110 (1993).
28. H.K. Kim and K.N. Tu, *Phys. Rev. B* 53, 16027 (1996).